Impact of Sparse Measurements in Freehand Setup for Antenna Characterization

G. Álvarez-Narciandi, J. Laviada, Y. Álvarez-López and F. Las-Heras
Dept. of Electrical Engineering
University of Oviedo
Gijón, Spain
alvareznguillermo@uniovi.es, laviadajaime@uniovi.es, alvarezyuri@uniovi.es, flasheras@uniovi.es

***Abstract*—The aim of the paper is to assess the quality of the obtained results using a portable system to perform antenna diagnostics versus acquisition time. The system comprises a handheld probe antenna, a motion capture system to track its position and a laptop to process the acquired data. The probe antenna is arbitrarily moved in front of the antenna under test (AUT) aperture, acquiring its near-field (NF) while its position is measured. The obtained data is processed in real-time using the Sources Reconstruction Method (SRM) to compute an equivalent currents distribution on the aperture of the AUT. Furthermore, a near-field to far-field (NF-FF) transformation is performed to retrieve the far-field radiation pattern of the AUT from the computed equivalent currents distribution. Specifically, the system was evaluated at 32 GHz using a vector network analyzer to measure the NF radiated by the AUT. The obtained results show that a scan of only a few seconds can provide a fast diagnostic of the AUT.**

I. Introduction

The advances in radiofrequency technology and the development of 5G networks and devices have entailed the popularization of higher frequency bands (e.g. 28 or 38 GHz) and the use of arrays, which comprise a large number of antennas in order to implement diversity and beamforming techniques [1]. Therefore, the ability to perform fast in-situ antenna diagnostics is of great importance due to the complexity of these antennas [2], [3], [4], [5]. In this regard, a system that employs an unmanned air vehicle to evaluate the performance of the antennas of base stations has been recently presented [6]. In this paper a novel portable system to perform antenna diagnostics is proposed. The system comprises a handheld probe antenna, a cost-effective highly accurate motion capture system to track its position and a laptop to process the acquired data. The probe antenna is arbitrarily moved by the operator of the system in front of the antenna under test (AUT) aperture, acquiring its near-field (NF) while its position is measured. The obtained data is processed in real-time using the Sources Reconstruction Method (SRM) to compute an equivalent currents distribution on the aperture of the AUT [7]. Furthermore, a near-field to far-field (NF-FF) transformation is performed to retrieve the far-field radiation pattern of the AUT from the computed equivalent currents distribution. The obtained information is updated in real-time and displayed to the operator of the system, so that NF acquisitions in undersampled areas can be further performed until enough data is gathered. In particular, the quality of the obtained results versus acquisition time, i.e., the number of NF and probe position measurements, is discussed comparing several snapshots of the equivalent currents distribution and the radiation pattern of the AUT during a scan.

II. System description

The portable setup for performing antenna diagnostics and characterization, depicted in Fig. 1, comprises the following parts:

- A handheld probe antenna used to capture the field radiated by the antenna under test.
- A Vector Network Analyzer (VNA) which measures both the amplitude and phase of the signal radiated by the AUT captured by the probe antenna.
- An optical tracking system that accurately computes the position of the probe antenna.
- A conventional laptop in charge of controlling field and position acquisitions and processing the measured data.

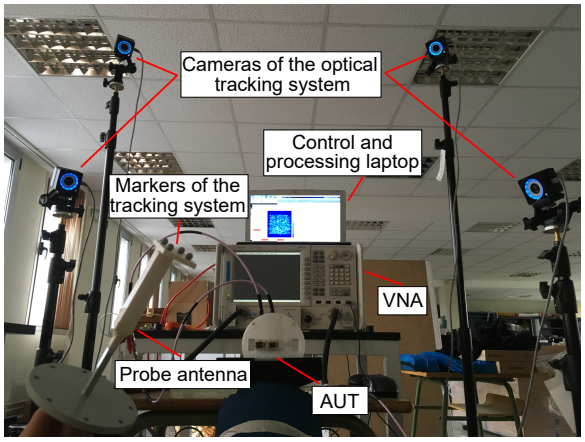

Fig. 1: Measurement setup of the proposed system.

The flowchart of the system, summarized in Fig. 2, is described below. First, there is an initialization step in which a virtual reference plane in front of the antenna under test is defined. This reference plane (XY-plane) is then discretized in a regular grid and a maximum number of samples per cell of the grid, N_{max}, is set. Finally, each cell of the grid is used as the base of a rectangular prism of a given height,

h. The value of the height of the rectangular prisms is a tolerance (in the z-axis) that allows the operator of the system to move in a comfortable manner the probe antenna with their hand in front of the antenna aperture while ensuring a proper sampling avoiding electrically large gaps between adjacent samples. It is relevant to observe that these deviations from the reference plane are taken into account by the SRM in order to compensate them. Next, the scan begins as the operator moves the probe antenna with their hand in front of the aperture of the antenna under test. During that movement, NF and position acquisitions are triggered by the control laptop. After a set of N_{block} NF and position acquisitions is performed, the data is processed using the SRM to compute an equivalent currents distribution at the aperture of the antenna under test. Then, the far-field pattern of the antenna under test is computed from the equivalent currents distribution by means of a NF-FF transformation. Finally, the updated information is displayed to the operator in order to decide whether enough information has been acquired. Besides, a heatmap depicting where measurements were taken within the grid of the reference plane is also displayed so that the operator can detect undersampled areas.

It should be noted that processing of the acquired data and the scan of the field of the antenna under test take place concurrently, i.e., an equivalent currents distribution and the far-field pattern of the AUT are computed using the gathered data from previous blocks at the same time that additional measurement data is acquired.

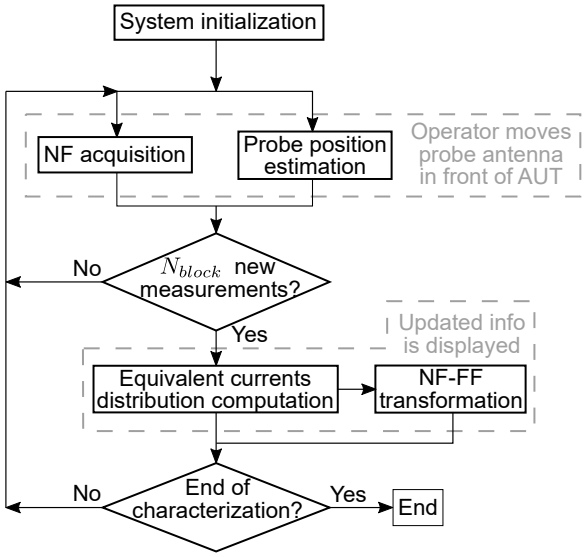

Fig. 2: Workflow of the proposed system.

III. Results

The performance of the system was evaluated by measuring a two-horn antenna array at 32 GHz. The AUT was connected to one port of a VNA and an open-ended waveguide, which was used as probe antenna, was connected to other port of the VNA. It should be pointed out that a portable VNA or a coherent detector could be used to acquire the amplitude and phase of the NF of the AUT. The position of the probe antenna was tracked employing the motion capture system of Optitrack using four infrared cameras and four reflective markers attached to the probe antenna. The size of the cells of the reference plane was set to 2×2 mm, the tolerance h was set to 2 cm and the maximum number of samples per cell of the grid was set to $N_{max} = 5$.

The AUT was scanned taking measurements moving the probe at an average distance of 6.1 cm from the AUT aperture. During the measurements a total of 1766 acquisitions were performed during 222 seconds. The normalized amplitude and phase of the acquired near-field samples are depicted in Figs. 3a and 3b, respectively.

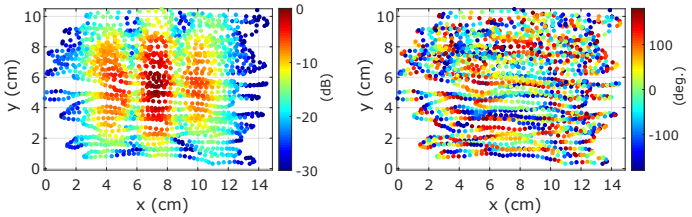

Fig. 3: Normalized amplitude (a) and phase (b) of the acquired near-field samples.

The obtained results, using all of the acquired measurements and the partial results obtained for two different snapshots during the scanning process are summarized in Fig. 4. The results retrieved using the first 400 samples that were acquired are outlined from Fig. 4a to Fig. 4d. The acquisition time of this 400 samples, measured at the positions depicted in Fig. 4a, was 49 seconds. The normalized amplitude and phase of the computed equivalent currents distribution are depicted in Fig. 4b and 4c, respectively. As it can be seen, although the existence of the two sources (each of them corresponding to one horn antenna) can be inferred, the currents at the aperture of the AUT (depicted in black dashed line) are not well defined, specially in the vertical direction (y-axis) as most of the measurements were acquired in the upper part of the aperture at that snapshot. The H-plane cut retrieved after performing the NF-FF transformation is depicted in Fig. 4d. As it can be observed, although the shape of the cut can be inferred, the side lobes are not accurately recovered.

The obtained results at the second snapshot of the scan, which were computed using the first 800 samples are outlined from Fig. 4e to Fig. 4h. The acquisition time of these 800 samples measured at the positions which are depicted in Fig. 4e was 95 seconds. The normalized amplitude and phase of the computed equivalent currents distribution are depicted in Fig. 4f and 4g, respectively. As it can be observed, the aperture of each horn is clearly characterized from its current distribution and its size is similar to the actual size of the horn aperture, although some artifacts still appear. The H-plane cut computed by performing a NF-FF transformation is depicted in Fig. 4h. As it can be observed, the retrieved cut is in agreement with

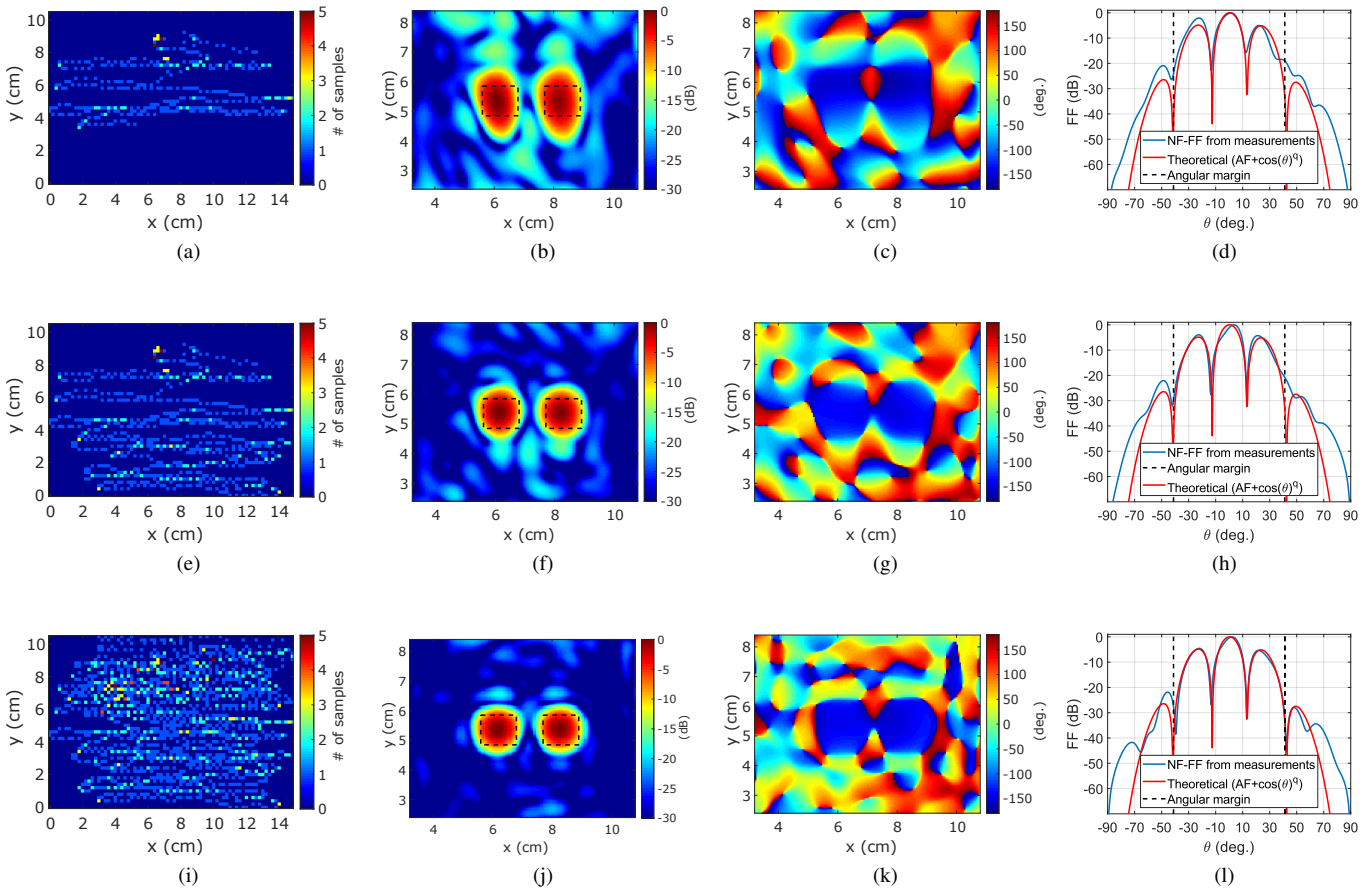

Fig. 4: Heatmap depicting the acquisition positions of the first 400 samples acquired during the scan (a), normalized amplitude (b) and phase (c) of the equivalent currents distribution computed with those samples, and H-plane cut of the far-field pattern obtained after NF-FF transformation (d). The same information is presented from (e) to (h) for a snapshot after 800 samples were acquired. Finally, the results obtained using all of the acquired measurements (1766 samples) is shown from (i) to (l).

the reference one, although the main lobe direction is slightly deviated (3.5°).

Finally, the results using all the acquired measurements are shown from Fig. 4i to Fig. 4l. The normalized amplitude and phase of the computed equivalent currents distribution are depicted in Fig. 4j and 4k, respectively. As it can be seen, the sources distribution corresponding to each horn can be clearly distinguished, their size is similar to physical dimensions of the antenna aperture and the noise level is reduced. Also, the difference between the amplitude and phase of each horn is only of 0.13 dB and 4.6°, respectively. The retrieved H-plane cut is depicted in Fig. 4l as well as the theoretical pattern. It should be pointed out that the theoretical pattern was obtained considering an array of two elements separated the same distance as the actual two-horn antenna array, which were fed with the same amplitude and phase and considering a $cos(\theta)^5$ pattern for each element. As can be observed, the retrieved pattern is similar to the theoretical one within the angular margin of validity of a planar range.

IV. Conclusions

A novel portable system to perform antenna diagnostics has been presented. The system is based on moving a handheld probe antenna in front of the AUT aperture while its position is tracked by a motion capture system and NF samples are acquired using a VNA. The obtained measurements are processed in real-time using the SRM algorithm to compute an equivalent currents distribution on the aperture of the AUT. In addition, a near-field to far-field (NF-FF) transformation is performed to retrieve the far-field radiation pattern of the AUT from the computed equivalent currents distribution.

The performance of the system was tested at 32 GHz by measuring a two-horn antenna array. Results show that the system is capable of assessing the performance of the AUT, enabling antenna diagnostics capabilities (e.g. detecting malfunctioning elements if present). In particular, the accuracy of the system versus the acquisition time was discussed comparing several snapshots of the equivalent currents distribution and the radiation pattern of the AUT at different moments of the scan. The obtained results show that a scan of only a few seconds can provide a fast diagnostics of the AUT. In conclusion, the presented system can assess, in-situ and rapidly, the performance of antennas, although it is not intended to replace laboratory measurement facilities when an exhaustive characterization is required. Future work involves

further development of this system in order to use amplitude-only data and a power detector.

ACKNOWLEDGEMENT

This work has been supported by the Ministerio de Educación y Formación Profesional of Spain under the FPU grant FPU15/06431, by the Ministerio de Ciencia, Innovación y Universidades under project RTI2018-095825-B-I00 and by the Principado de Asturias/FEDER under project IDI/2018/000191.

REFERENCES

[1] P. Demestichas, A. Georgakopoulos, D. Karvounas, K. Tsagkaris, V. Stavroulaki, J. Lu, C. Xiong, and J. Yao, "5G on the Horizon: Key Challenges for the Radio-Access Network," *IEEE Vehicular Technology Magazine*, vol. 8, no. 3, pp. 47–53, Sep. 2013.

[2] O. M. Bucci, A. Capozzoli, and G. D'Elia, "Diagnosis of array faults from far-field amplitude-only data," *IEEE Transactions on Antennas and Propagation*, vol. 48, no. 5, pp. 647–652, May 2000.

[3] J. A. Rodriguez-Gonzalez, F. Ares-Pena, M. Fernandez-Delgado, R. Iglesias, and S. Barro, "Rapid method for finding faulty elements in antenna arrays using far field pattern samples," *IEEE Transactions on Antennas and Propagation*, vol. 57, no. 6, pp. 1679–1683, June 2009.

[4] G. Oliveri, P. Rocca, and A. Massa, "Reliable diagnosis of large linear arraysa bayesian compressive sensing approach," *IEEE Transactions on Antennas and Propagation*, vol. 60, no. 10, pp. 4627–4636, Oct 2012.

[5] M. D. Migliore, "A compressed sensing approach for array diagnosis from a small set of near-field measurements," *IEEE Transactions on Antennas and Propagation*, vol. 59, no. 6, pp. 2127–2133, June 2011.

[6] M. G. Fernandez, Y. A. Lopez, and F. Las-Heras, "On the use of unmanned aerial vehicles for antenna and coverage diagnostics in mobile networks," *IEEE Communications Magazine*, vol. 56, no. 7, pp. 72–78, July 2018.

[7] Y. Alvarez, F. Las-Heras, and M. R. Pino, "Reconstruction of equivalent currents distribution over arbitrary three-dimensional surfaces based on integral equation algorithms," *IEEE Transactions on Antennas and Propagation*, vol. 55, no. 12, pp. 3460–3468, Dec 2007.